

# Host–Guest Interactions of Inorganic Phosphates with the Copper(II) Complexes of the Hexaaza Macrocyclic Ligand

## 3,6,9,17,20,23-Hexaazatriacyclo[23.3.1.1<sup>11,15</sup>]triaconta-1(29),11(30),12,14,25,27-hexaene

David A. Nation, Arthur E. Martell,\* Richard I. Carroll, and Abraham Clearfield

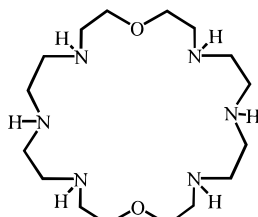
Department of Chemistry, Texas A&M University, College Station, Texas 77843-3255

Received June 5, 1996<sup>⊗</sup>

The host–guest interactions between ortho-, pyro-, and tripolyphosphate anions and the mono and dinuclear copper(II) complexes of the hexaaza macrocyclic ligand BMXD (3,6,9,17,20,23-hexaazatriacyclo[23.3.1.1<sup>11,15</sup>]triaconta-1(29),11(30),12,14,25,27-hexaene) were investigated by potentiometric equilibrium methods. Ternary complexes are formed in aqueous solution as a result of coordinate bonding, hydrogen bond formation, and Coulombic attraction between the host and guest. Formation constants for all the species found are reported. The dinuclear copper(II) complexes of BMXD show strong selectivity for pyrophosphate ions in the presence of orthophosphate ions over the whole p[H] range; the pyrophosphate/tripolyphosphate selectivity is p[H] dependent. The dinuclear copper(II) complex of BMXD, (Cu<sub>2</sub>-BMXD)(SO<sub>4</sub>)<sub>2</sub>, crystallizes in the orthorhombic space group *Pccn*, with *a* = 15.73(2) Å, *b* = 20.27(1) Å, *c* = 9.045(5) Å, and *Z* = 4. The sulfate counterions are found to bridge the copper(II) ions in adjacent molecules leading to an extended polymeric structure.

### Introduction

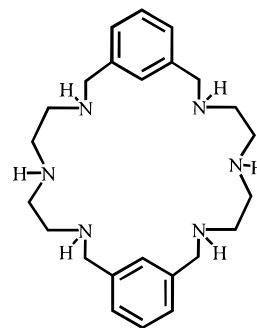
Polyaza macrocyclic ligands, in their protonated forms, have been shown to bind certain neutral molecules and anions in solution<sup>1–4</sup> and, in some instances, are able to catalyze biologically significant reactions of the bound substrates.<sup>5–7</sup> Often these enzyme-mimetic reactions show enhanced rate factors when compared with the same process in the absence of the macrocycle. In addition, hexaaza macrocycles can form mono and dinuclear metal complexes which in turn are capable of coordinating anions.<sup>3,4,8,9</sup> In the case of dinuclear cobalt(II) complexes of OBISDIEN, **1**, the oxidation of inorganic and



OBISDIEN, **1**

tion of the substrate and molecular oxygen to the two metal centers.<sup>10,11</sup> Other reaction types, such as ATP hydrolysis and formation, have been investigated with a variety of ligands and metal ions.<sup>6,12</sup> The investigation of macrocyclic ligands and their metal complexes can lead to a better understanding of certain biological functions as well as to new catalysts of value in chemical synthesis.

Recently the complexes formed between the various protonated forms of the hexaaza macrocyclic ligand 3,6,9,17,20,23-hexaazatriacyclo[23.3.1.1<sup>11,15</sup>]triaconta-1(29),11(30),12,14,25,27-hexaene (BMXD), **2**, and the series of anions derived from



BMXD, **2**

organic anions has been achieved by the simultaneous coordina-

tion of phosphoric, diphosphoric, and triphosphoric acid were reported.<sup>13</sup> Stable binary complexes were formed as a result of Coulombic attraction and hydrogen bond formation, with the strength of interaction increasing in the order mono- < di- < tripolyphosphate. These results were related to other studies involving the biologically relevant substrate adenosine-5'-triphosphate, ATP, and the hexaaza macrocycle OBISDIEN.<sup>7</sup>

<sup>⊗</sup> Abstract published in *Advance ACS Abstracts*, November 15, 1996.

- (1) Aguilar, J. A.; García-España, E.; Guerrero, J. A.; Luis, S. V.; Llinares, J. M.; Miravet, J. F.; Ramírez, J. A.; Soriano, C. *J. Chem. Soc., Chem. Commun.* **1995**, 2237.
- (2) Lu, Q.; Motekaitis, R. J.; Reibenspies, J. H.; Martell, A. E. *Inorg. Chem.* **1995**, *34*, 4958.
- (3) Llobet, A.; Reibenspies, J. H.; Martell, A. E. *Inorg. Chem.* **1994**, *33*, 5946.
- (4) Motekaitis, R. J.; Martell, A. E. *Inorg. Chem.* **1992**, *31*, 5534.
- (5) Andrés, A.; Aragón, J.; Bencini, A.; Bianchi, A.; Domenech, A.; Fusi, V.; García-España, E.; Paoletti, P.; Ramírez, J. A. *Inorg. Chem.* **1993**, *32*, 3418.
- (6) Bencini, A.; Bianchi, A.; Garcia-Espana, E.; Scott, E. C.; Morales, L.; Wang, B.; Deffo, T.; Takusagawa, F.; Mertes, M. P.; Mertes, K. B.; Paoletti, P. *Bioorg. Chem.* **1992**, *20*, 8.
- (7) Hosseini, M. W.; Lehn, J.-M. *Helv. Chim. Acta* **1987**, *70*, 1312.
- (8) Fabbri, L.; Pallavicini, P.; Parodi, L.; Perotti, A.; Taglietti, A. *J. Chem. Soc., Chem. Commun.* **1995**, 2439.
- (9) Jurek, P. E.; Martell, A. E.; Motekaitis, R. J.; Hancock, R. D. *Inorg. Chem.* **1995**, *34*, 1823.

- (10) Motekaitis, R. J.; Martell, A. E. *Inorg. Chem.* **1994**, *33*, 1032.
- (11) Rosso, N. D.; Szpogancz, B.; Motekaitis, R. J.; Martell, A. E. *Inorg. Chim. Acta* **1994**, *227*, 49.
- (12) Hosseini, M. W.; Lehn, J.-M. *J. Chem. Soc., Chem. Commun.* **1991**, 451.
- (13) Nation, D. A.; Reibenspies, J. H.; Martell, A. E. *Inorg. Chem.* **1996**, *35*, 4597.

The ligand BMXD, **2**, consisting of two diethylenetriamine moieties separated by *m*-xylyl bridges, is capable of forming mono as well as dinuclear metal complexes, whereby each metal ion is coordinated by three amino nitrogen atoms leaving additional coordination sites available. In aqueous solution these coordination sites could be occupied by H<sub>2</sub>O, OH<sup>−</sup>, or anionic substrates. The formation of mono and dinuclear copper(II) complexes of BMXD has been previously reported<sup>14</sup> but thus far no accounts of additional substrate binding by these complexes have been described. In continuation of our work on molecular recognition and catalysis, the binding of the anionic substrates phosphate, diphosphate (pyrophosphate), and tripolyphosphate by the mono and dinuclear copper(II) complexes of BMXD are now reported. Potentiometric equilibrium methods are employed successfully to elucidate the nature of the ternary species formed in solution. These results are then compared with those obtained in the absence of metal ions. Additionally the X-ray crystal structure of the dinuclear copper(II) complex of BMXD, (Cu<sub>2</sub>-BMXD)(SO<sub>4</sub>)<sub>2</sub>, is reported.

## Experimental Section

**Materials.** The ligand BMXD was prepared as a colorless hexahydrobromide salt according to a published procedure.<sup>14</sup> GR grade KCl was obtained from EM Chemical Co. and CO<sub>2</sub>-free Dilut-it ampoules of KOH were purchased from J. T. Baker Inc. Reagent grade potassium dihydrogenphosphate and tetrasodium pyrophosphate were purchased from Fisher Scientific Co. and were purified by recrystallization from distilled water. Sodium tripolyphosphate (technical grade, 85%) was purchased from Aldrich Chemical Co. and was purified by repeated crystallization from aqueous solution by the addition of methanol.<sup>15</sup> The KOH solution was standardized by titration against standard potassium acid phthalate with phenolphthalein as indicator and was checked periodically for carbonate content (<2%).<sup>16</sup> The Cu<sup>2+</sup> solution was prepared from CuCl<sub>2</sub>·2H<sub>2</sub>O and was standardized with standard EDTA and 1-(2-pyridylazo)-2-naphthol (PAN) as indicator, according to Schwarzenbach.<sup>17</sup>

**Potentiometric Titrations.** Potentiometric measurements were conducted in a jacketed cell thermostated at 25.0 ± 0.1 °C and kept under an inert atmosphere of purified argon. A Corning Model 350 pH meter fitted with glass and calomel reference electrodes was used. KCl was employed as supporting electrolyte to maintain the ionic strength at 0.10 M. The apparatus was calibrated in terms of  $-\log\{[H^+]\}$ , designated as p[H], by titration of a small quantity of dilute HCl at 0.10 M ionic strength and 25.0 °C followed by adjustment of the meter so as to minimize the calculated p[H] vs observed values. Log *K*<sub>w</sub> for the system, defined in terms of  $\log\{[H^+][OH^-]\}$ , was found to be  $-13.78$  at the ionic strength employed<sup>18</sup> and was maintained fixed during refinements.

Potentiometric measurements of solutions containing equimolar amounts of BMXD and the appropriate phosphate anion, along with 1 or 2 equiv of Cu<sup>2+</sup>, were made at concentrations of approximately 1 × 10<sup>−3</sup> M (in BMXD) and ionic strength  $\mu = 0.10$  M (KCl). Each titration utilized at least 10 points per neutralization of a hydrogen ion equivalent with titrations being repeated until satisfactory agreement was obtained. A minimum of three sets of data were used in each case to calculate the overall stability constants and their standard deviations. The range of accurate p[H] measurement was considered to be 2–12. Equilibrium constants and species distribution diagrams were calculated using the programs BEST and SPE respectively.<sup>16</sup>

The protonation constants of BMXD and the series of phosphate anions, as well as the formation constants of the binary species formed between BMXD and the phosphate anions, have been previously determined under the same experimental conditions as used in this work.<sup>13</sup>

**Crystal Structure Determination. Preparation of (Cu<sub>2</sub>-BMXD)(SO<sub>4</sub>)<sub>2</sub>.** Tiny blue crystals of the dinuclear copper(II) complex were obtained by the slow diffusion of acetone into an aqueous solution of BMXD·6HBr and CuSO<sub>4</sub>·2H<sub>2</sub>O in 1:2 molar ratio that had been adjusted to p[H] 6.3 with dilute KOH.

**Data Collection.** A blue needle crystal having approximate dimensions of 0.08 × 0.05 × 0.20 mm was mounted on a glass fiber. All measurements were made on a Rigaku AFC5R diffractometer with graphite monochromated Cu Kα radiation and a rotating anode generator operated at 50 kV and 180 mA.

Cell constants and an orientation matrix for data collection, obtained from a least-squares refinement using the setting angles of 12 carefully centered reflections in the range 43.68 < 2θ < 56.86°, corresponded to a primitive orthorhombic cell. The systematic absences of

$$0kl: l \neq 2n$$

$$h0l: l \neq 2n$$

$$hk0: h + k \neq 2n$$

uniquely defined the space group to be *Pccn* (No. 56).

The data were collected at a temperature of  $-110 \pm 2$  °C using the  $\omega$ -2θ scan technique to a maximum 2θ value of 120°. The  $\omega$  scans of several intense reflections, made prior to data collection, had an average width at half-height of 0.37° with a take-off angle of 6.0°. Scans of  $(1.37 + 0.30 \tan \theta)^\circ$  were made at a speed of 4.0°/min (in  $\omega$ ). The weak reflections ( $I < 10.0\sigma(I)$ ) were rescanned (maximum of three scans) and the counts were accumulated to ensure good counting statistics. Stationary background counts were recorded on each side of the reflections. The ratio of peak counting time to background counting time was 2:1. The diameter of the incident beam collimator was 0.5 mm, the crystal to detector distance was 285 mm, and the detector aperture was 9.0 × 13.0 mm (horizontal × vertical).

**Data Reduction.** A total of 2329 reflections were scanned, of which only 989 had  $I > 3\sigma$ , probably due to the small size of the crystal. The intensities of three representative reflections were measured after every 150 reflections. A linear decay of 1.2% in the standard reflections was observed and corrected for. The linear absorption coefficient,  $\mu$ , for Cu Kα radiation is 36.8 cm<sup>−1</sup>. An empirical absorption correction based on azimuthal scans of three reflections was applied, which resulted in transmission factors ranging from 0.83 to 1.00. The data were corrected for Lorentz and polarization effects.

**Structure Solution and Refinement.** The structure was solved by direct methods<sup>19</sup> and expanded using Fourier techniques.<sup>20</sup> Only the Cu, S, O, and N atoms were refined anisotropically, while the rest were refined isotropically because of the limited number of reflections. Hydrogen atoms were included but not refined. The final cycle of full-matrix least-squares refinement<sup>21</sup> was based on 989 observed reflections ( $I > 3.00\sigma(I)$ ) and 130 variable parameters and converged (largest parameter shift was 0.03 times its esd) with unweighted and weighted agreement factors of 0.07 and 0.061, respectively.

The standard deviation of an observation of unit weight<sup>22</sup> was 2.17. The weighting scheme was based on counting statistics and included a factor ( $p = 0.010$ ) to downweight the intense reflections. Plots of

(14) Menif, R.; Martell, A. E.; Squattrito, P. J.; Clearfield, A. *Inorg. Chem.* **1990**, *29*, 4723.

(15) Waters, J. I.; Loughran, E. D.; Lambert, S. M. *J. Am. Chem. Soc.* **1956**, *78*, 4855.

(16) Martell, A. E.; Motekaitis, R. J. *Determination and Use of Stability Constants*, 2nd ed.; VCH Publishers: New York, 1992.

(17) Schwarzenbach, G.; Flaschka, H. *Complexometric Titrations*, 2nd ed.; Methuen: London, 1969.

(18) Smith, R. M.; Martell, A. E. *NIST Critically Selected Stability Constants: Version 2.0*, National Institute of Standards and Technology: Gaithersburg, MD, 1995.

(19) Altomare, A.; Burla, M. C.; Camalli, M.; Cascarano, M.; Giacovazzo, C.; Guagliardi, A.; Polidori, G. *J. Appl. Crystallogr.* **1994**, *3*, 435.

(20) Beurskens, P. T.; Admiraal, G.; Beurskens, G.; Bosman, W. P.; Garcia-Granda, S.; Gould, R. O.; Smits, J. M. M.; Smykalla, C. *The DIRDAF program system, Technical Report of the Crystallography Laboratory*; University of Nijmegen: Nijmegen, The Netherlands; 1992.

(21) Least-squares methods were used. Function minimized:  $\sum w(|F_o| - |F_c|)^2$ , where  $w = 1/\sigma^2(F_o) = 4F_o^2/\sigma^2(F_o^2)$ ,  $\sigma^2(F_o^2) = [S^2(C + R^2B) + (pF_o^2)^2]/(Lp)^2$ ,  $S$  = scan rate,  $C$  = total integrated peak count,  $R$  = ratio of scan time to background counting time,  $B$  = total background count,  $Lp$  = Lorentz-polarization factor, and  $p = p$  factor

(22) Standard deviation of an observation of unit weight:  $[\sum w(|F_o| - |F_c|)^2 / (N_o - N_v)]^{1/2}$  where  $N_o$  = number of observations and  $N_v$  = number of variables.

**Table 1.** Copper(II) Binding Constants of the Hexaazamacrocyclic BMXD (L = BMXD, Charges Have Been Omitted for Clarity)

symbol	equilibrium quotient, $K$	$\log K^a$	$\log K^b$
$K_{ML}^M$	$[ML]/[M][L]$	13.63(8)	13.79
$K_{MHL}^H$	$[MHL]/[ML][H]$	8.40(2)	8.69
$K_{MH_2L}^H$	$[MH_2L]/[MHL][H]$	7.20(6)	7.32
$K_{MH_3L}^H$	$[MH_3L]/[MH_2L][H]$	3.68(1)	
$K_{M(OH)L}^{OH}$	$[M(OH)L]/[H]/[ML]$	-8.93(2)	
$K_{M(OH)_2L}^{OH}$	$[M(OH)_2L]/[H]/[M(OH)L]$	-11.48(4)	
$K_{M_2L}^M$	$[M_2L]/[ML][M]$	10.86(6)	9.68
$K_{M_2(OH)L}^{OH}$	$[M_2(OH)L]/[H]/[M_2L]$	-7.83(3)	-7.26
$K_{M_2(OH)_2L}^{OH}$	$[M_2(OH)_2L]/[H]/[M_2(OH)L]$	-8.74(1)	-8.40
$K_{M_2(OH)_3L}^{OH}$	$[M_2(OH)_3L]/[H]/[M_2(OH)_2L]$	-11.70(10)	

<sup>a</sup> This work, 25.0 °C,  $\mu = 0.10$  M (KCl) (standard deviations in parentheses). <sup>b</sup> Reference 14, 25.0 °C,  $\mu = 0.10$  M (KNO<sub>3</sub>).

$\sum w(|F_o| - |F_c|)^2$  vs  $|F_o|$ , reflection order in data collection,  $(\sin \theta)/\lambda$ , and various classes of indices showed no unusual trends. The maximum and minimum peaks in the final difference Fourier map corresponded to +0.70 and -0.66 e/Å<sup>3</sup>, respectively.

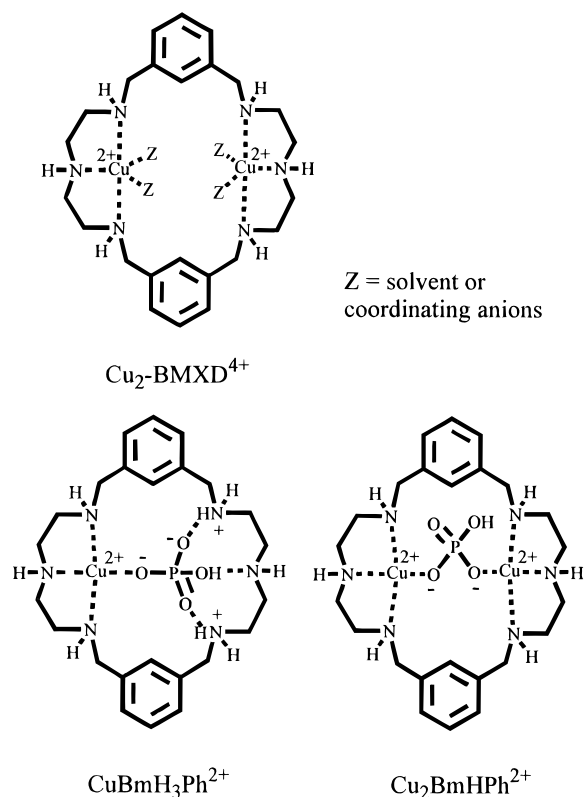
Neutral atom scattering factors were taken from Cromer and Waber.<sup>23</sup> Anomalous dispersion effects were included in  $F_c$ ;<sup>24</sup> the values for  $\Delta f'$  and  $\Delta f''$  were those of Creagh and McAuley.<sup>25</sup> The values for the mass attenuation coefficients are those of Creagh and Hubbel.<sup>26</sup> All calculations were performed with the TEXSAN<sup>27</sup> crystallographic software package of Molecular Structure Corp.

## Results and Discussion

**Copper Complex Stability Studies of BMXD.** Copper(II) ions have been shown to form both 1:1 and 1:2 ligand to metal complexes with BMXD.<sup>14</sup> In that work different experimental conditions were employed; therefore, the redetermination of the stability constants was necessary for this study. Table 1 compares the results of this work with the literature values. It can be seen that fairly close agreement is obtained for the log stability constants of those species that are common to both this and the previous study. The small differences, and the detection of further species in this study, may be a result of the use of different supporting electrolytes in each case. In this work KCl was employed as the supporting electrolyte. The effect, if any, that the presence of chloride ion has on the stability of the mono- and dinuclear copper(II) complexes is incorporated into the magnitude of their stability constants as given in Table 1. During calculation of the association constants between the copper(II) complexes and the polyphosphate anions, the constants of Table 1 are subtracted from the overall formation constants of the ternary species, thus negating the effects of chloride ion.

The coordination geometry of the copper(II) ions in the dinuclear complex cation Cu<sub>2</sub>-BMXD<sup>4+</sup> has been previously suggested<sup>14</sup> and is shown schematically in Chart 1. This structural arrangement has now been confirmed by X-ray crystallography.

**Crystal and Molecular Structure of (Cu<sub>2</sub>-BMXD)(SO<sub>4</sub>)<sub>2</sub>.** The structure of the dinuclear copper(II) complex of BMXD

**Chart 1****Table 2.** Summary of Crystal Data Collection and Refinement Parameters for (Cu<sub>2</sub>-BMXD)(SO<sub>4</sub>)<sub>2</sub>

empirical formula	Cu <sub>2</sub> C <sub>24</sub> N <sub>6</sub> O <sub>8</sub> H <sub>38</sub> S <sub>2</sub>
fw	729.81
space group	<i>Pccn</i> (No. 56)
<i>a</i> , Å	15.73(2)
<i>b</i> , Å	20.27(1)
<i>c</i> , Å	9.045(5)
<i>Z</i>	4
<i>V</i> , Å <sup>3</sup>	2882(3)
<i>D</i> <sub>calc</sub> , g/cm <sup>3</sup>	1.682
temp, K	163(2)
$\mu$ (Cu K $\alpha$ ), cm <sup>-1</sup>	36.81
$\lambda$ , Å	1.54178
reflection to param ratio	7.6
no. of variables	130
max. and min. transm factors	0.8277–0.9986
residuals: <i>R</i> ; <i>R</i> <sub>w</sub> <sup>a</sup>	0.070; 0.061
largest diff peak and hole, e Å <sup>-3</sup>	0.70 and -0.66

<sup>a</sup>  $R = \sum ||F_o| - |F_c|| / \sum |F_o|$ .  $R_w = [(\sum w(|F_o| - |F_c|)^2) / \sum w F_o^2]^{1/2}$ .  $w = 1/\sigma^2(F_o) = 4F_o^2/\sigma^2(F_o^2)$ .

was determined by X-ray methods. A summary of the data collection and refinement parameters is given in Table 2. A table of selected bond lengths and angles is given in Table 3. Tables of atomic coordinates and thermal displacement parameters are contained in the Supporting Information section.

The structure of (Cu<sub>2</sub>-BMXD)(SO<sub>4</sub>)<sub>2</sub>, showing the atomic numbering scheme, is indicated in Figure 1. The molecule possesses a center of symmetry which transposes one half of the molecule into the other. Each macrocycle binds two copper(II) ions by way of its diethylenetriamine moieties which provide three nitrogen donors to each metal ion. The coordination set around the copper ion is completed by the coordination of one sulfate oxygen atom (O(3)) in an equatorial position and another sulfate oxygen atom (O(4')), from a different sulfate anion, in an apical position, thus resulting in a distorted square pyramidal geometry. The Cu–N bond distances range from 1.99(1) to

(23) Cromer, D. T.; Waber, J. T. *International Tables for X-ray Crystallography*; The Kynoch Press: Birmingham, England, 1974; Vol. IV, Table 2.2 A.

(24) Ibers, J. A.; Hamilton, W. C. *Acta Crystallogr.* **1964**, *17*, 781.

(25) Creagh, D. C.; McAuley, W. J. *International Tables for X-ray Crystallography*; Wilson, A. J. C., Ed.; Kluwer Academic Publishers: Boston, MA, 1992; Vol. C, Table 4.2.6.8, pp 219–222.

(26) Creagh, D. C.; Hubbel, J. H. *International Tables for X-ray Crystallography*; Wilson, A. J. C., Ed.; Kluwer Academic Publishers: Boston, MA, 1992; Vol. C, Table 4.2.4.3, pp 200–206.

(27) TEXSAN: *Crystal Structure Analysis Package*; Molecular Structure Corporation: The Woodlands, TX, 1985 and 1992.

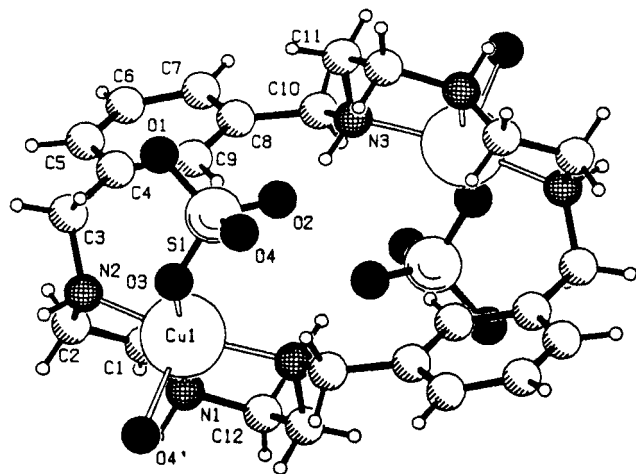


**Figure 1.** Diagram of  $(\text{Cu}_2\text{-BMXD})(\text{SO}_4)_2$  showing the atomic numbering scheme. Hydrogen atoms have been placed in calculated positions.

**Table 3.** Selected Bond Lengths (Å) and Angles (deg) for  $(\text{Cu}_2\text{-BMXD})(\text{SO}_4)_2$  (Standard Deviations in Parentheses)

Cu(1)–O(3)	1.947(8)	Cu(1)–O(4)	2.262(10)
Cu(1)–N(1)	1.99(1)	Cu(1)–N(2)	2.06(1)
Cu(1)–N(3)	2.04(1)	S(1)–O(1)	1.477(9)
S(1)–O(2)	1.444(9)	S(1)–O(3)	1.511(9)
S(1)–O(4)	1.481(9)	Cu(1)–Cu(1')	5.31(1)
O(3)–Cu(1)–O(4)	87.0(4)	O(3)–Cu(1)–N(1)	176.2(5)
O(3)–Cu(1)–N(2)	92.1(4)	O(3)–Cu(1)–N(3)	97.8(4)
O(4)–Cu(1)–N(1)	91.4(4)	O(4)–Cu(1)–N(2)	100.9(4)
O(4)–Cu(1)–N(3)	95.4(4)	N(1)–Cu(1)–N(2)	84.7(5)
N(1)–Cu(1)–N(3)	85.9(4)	N(2)–Cu(1)–N(3)	161.3(5)
O(1)–S(1)–O(2)	112.3(7)	O(1)–S(1)–O(3)	107.7(6)
O(1)–S(1)–O(4)	110.0(6)	O(2)–S(1)–O(3)	109.0(6)
O(2)–S(1)–O(4)	110.6(6)	O(3)–S(1)–O(4)	107.0(5)
Cu(1)–O(3)–S(1)	131.7(6)	Cu(1)–O(4)–S(1)	120.6(5)

2.06(1) Å and are typical for interactions of this type.<sup>28–31</sup> The equatorial Cu–O bond distance is 1.947(8) Å while the axial Cu–O bond distance is considerably longer at 2.262(10) Å, consistent with the expected Jahn–Teller distortion.

Coordination of the sulfate anion to the metal center perturbs the usual tetrahedral symmetry of the anion. The oxygen atom that is bound equatorially to the copper ion has the longest S–O bond distance (1.511(9) Å) consistent with it being strongly coordinated to the metal. Coordination of the sulfate oxygen atom in the axial position of the copper ion has less effect on the sulfur–oxygen bond length and in fact the S(1)–O(4) bond distance is not very much different from that of S(1)–O(1), 1.481(9) and 1.477(9) Å, respectively, O(1) not being coordinated to anything. Because the sulfate anions bridge the two copper centers in neighboring molecules, the crystal has an extended polymeric structure.

Even though the solid state structure of  $(\text{Cu}_2\text{-BMXD})(\text{SO}_4)_2$  shows that the macrocycle adopts a chair type conformation, with one coordinating diethylene triamine moiety flipped down and the other flipped up, this is not necessarily the structure adopted in solution. It is expected that the cation would be able to attain a configuration where both diethylenetriamine moieties were flipped to the same side in order to accommodate larger bridging anions such as pyrophosphate.

The interatomic distance between the copper(II) ions within the same macrocycle is 5.31 Å. The copper(II) ions in a similar dinuclear macrocyclic complex have been found to be separated by a distance of 5.34 Å which, surprisingly, does not change upon incorporation of a bridging oxalate anion.<sup>32</sup> The incorporation of rigid aromatic spacers into the macrocyclic ring reduces the flexibility of such macrocycles and limits the accessible range of metal–metal interatomic distance.<sup>31</sup> This is not the case with ligands of the type OBISDIEN where the highly flexible macrocycle can accommodate metal ions with a variety of interatomic distances, with and without bridging anions.<sup>28</sup> Nevertheless, it was expected that the dinuclear copper complexes of BMXD may also be well suited to the incorporation of bridging anions of various size and charge.

**Guests of Copper Complexes of BMXD. Copper–BMXD–orthophosphate.** In previous work the interaction of orthophosphate ions with the protonated forms of BMXD was found to be fairly weak with only three association species being detected in the p[H] range 2–12.<sup>13</sup> In contrast, the mono- and dinuclear copper(II) complexes of BMXD are able to form a greater variety of association complexes with orthophosphate anion having, also, correspondingly greater stability constants, Table 4. A similar study with OBISDIEN and copper(II) found only six different ternary complex species even though it had been shown that OBISDIEN forms a greater number of binary complex species with orthophosphate than does BMXD.<sup>4</sup>

Coordinate bonding and Coulombic attraction between the negatively charged phosphate anion and the positively charged copper(II) complex, as well as the possibility of hydrogen-bonding interactions, lead to the formation of ternary species. The stability of the mononuclear ternary species, if one considers  $\text{PO}_4^{3-}$  as the substrate, increase as the degree of protonation of the mononuclear complex increases, up to a maximum found for  $\text{CuBmH}_3\text{Ph}^{2+}$ . Further protonation causes a fall in the formation constant by several orders of magnitude. This can be understood by considering that for the formation of  $\text{CuBmH}_4\text{-Ph}^{3+}$  to occur a proton must be added to  $\text{CuBmH}_3\text{Ph}^{2+}$ , shown in Chart 1. Whereas the increasing number of protonated amine nitrogen atoms led to an increase in possible hydrogen bonding sites the maximum number of such interactions was achieved in  $\text{CuBmH}_3\text{Ph}^{2+}$ . A further proton, added now to a phosphate oxygen atom, must cause the disruption of one of the oxygen to nitrogen hydrogen bonds and possibly weakens the coordinate bonding between the copper ion and the phosphate oxygen atom leading to a decrease in the stability of the product.

The magnitude of the formation constants for the ternary species formed between the orthophosphate anion and the dinuclear copper(II) BMXD complexes follow the trend that would be expected on electrostatic grounds. The binding mode of the orthophosphate ion to both  $\text{Cu}_2\text{Bm}(\text{OH})^{3+}$  and  $\text{Cu}_2\text{Bm}^{4+}$  would probably be the same in each case so the lower formation constant found for  $\text{Cu}_2\text{Bm}(\text{OH})\text{Ph}$  can be attributed to the lesser positive charge of the reacting species  $\text{Cu}_2\text{Bm}(\text{OH})^{3+}$  when compared to  $\text{Cu}_2\text{Bm}^{4+}$ . If the formation constants of the species  $\text{Cu}_2\text{BmPh}^+$ ,  $\text{Cu}_2\text{BmHPh}^{2+}$ , and  $\text{Cu}_2\text{BmH}_2\text{Ph}^{3+}$  are compared, it can be seen that the charge on the dinuclear complex remains the same but the negative charge of the phosphate substrate decreases with increasing protonation, thus lowering the electrostatic attraction between the reacting pairs. Another important consideration is that successive protonation of the orthophosphate anion changes and consequently weakens the coordinate bonding between it and the copper(II) centers. The suggested binding mode for the species  $\text{Cu}_2\text{BmHPh}^{2+}$  is shown in Chart

(28) Coughlin, P. K.; Lippard, S. J. *J. Am. Chem. Soc.* **1984**, *106*, 2328.

(29) Martin, A. E.; Lippard, S. J. *J. Am. Chem. Soc.* **1984**, *106*, 2579.

(30) O'Young, C.-L.; Dewan, J. C.; Lilienthal, H. R.; Lippard, S. J. *J. Am. Chem. Soc.* **1978**, *100*, 7291.

(31) Bazzicalupi, C.; Bencini, A.; Bianchi, A.; Fusi, V.; Giorgi, C.; Paoletti, P.; Stefani, A.; Valtancoli, B. *Inorg. Chem.* **1995**, *34*, 552.

(32) Lu, Q.; Motekaitis, R. J.; Reibenspies, J. H.; Martell, A. E. *Inorg. Chem.* **1996**, *35*, 2639.

**Table 4.** Overall Stability Constants and Stepwise Formation Constants for the Cu(II)–BMXD–Orthophosphate System (Bm = BMXD; Ph = PO<sub>4</sub><sup>3-</sup>; Charges Have Been Omitted for Clarity)

stoichiometry				log β <sup>a</sup>	equilibrium quotient, <i>K</i>	log <i>K</i>	equilibrium quotient, <i>K'</i> , involving principal species	log <i>K'</i>
Bm	Cu	Ph	H					
1	1	1	0	20.10(5)	[CuBmPh]/[CuBm][Ph]	6.47	[CuBmPh]/[CuBm(OH)][HPh]	3.90
1	1	1	1	28.95(3)	[CuBmHPh]/[CuBmH][Ph]	7.03	[CuBmHPh]/[CuBm][HPh]	3.82
1	1	1	2	37.55(5)	[CuBmH <sub>2</sub> Ph]/[CuBmH <sub>2</sub> ][Ph]	8.37	[CuBmH <sub>2</sub> Ph]/[CuBmH][HPh]	4.13
1	1	1	3	45.00(2)	[CuBmH <sub>3</sub> Ph]/[CuBmH <sub>3</sub> ][Ph]	12.10	[CuBmH <sub>3</sub> Ph]/[CuBmH <sub>2</sub> ][HPh]	4.32
1	1	1	4	50.74(5)	[CuBmH <sub>4</sub> Ph]/[CuBmH <sub>4</sub> ][HPh]	6.34	[CuBmH <sub>4</sub> Ph]/[CuBmH <sub>2</sub> ][H <sub>2</sub> Ph]	3.30
1	2	1	-1	23.62(7)	[Cu <sub>2</sub> Bm(OH)Ph]/[Cu <sub>2</sub> Bm(OH)][Ph]	6.97	[Cu <sub>2</sub> Bm(OH)Ph]/[Cu <sub>2</sub> Bm(OH) <sub>2</sub> ][HPh]	4.20
1	2	1	0	32.36(3)	[Cu <sub>2</sub> BmPh]/[Cu <sub>2</sub> Bm][Ph]	7.88	[Cu <sub>2</sub> BmPh]/[Cu <sub>2</sub> Bm(OH)][HPh]	4.21
1	2	1	1	40.47(3)	[Cu <sub>2</sub> BmHPh]/[Cu <sub>2</sub> Bm][HPh]	4.49	[Cu <sub>2</sub> BmHPh]/[Cu <sub>2</sub> Bm][HPh]	4.49
1	2	1	2	45.89(4)	[Cu <sub>2</sub> BmH <sub>2</sub> Ph]/[Cu <sub>2</sub> Bm][H <sub>2</sub> Ph]	3.15	[Cu <sub>2</sub> BmH <sub>2</sub> Ph]/[Cu <sub>2</sub> Bm][H <sub>2</sub> Ph]	3.15

<sup>a</sup> μ = 0.10 M (KCl); 25.0 °C (standard deviations in parentheses).

**Table 5.** Overall Stability Constants and Stepwise Formation Constants for the Cu(II)–BMXD–Pyrophosphate System (Bm = BMXD; Py = P<sub>2</sub>O<sub>7</sub><sup>4-</sup>; Charges Have Been Omitted for Clarity)

stoichiometry				log β <sup>a</sup>	equilibrium quotient, <i>K</i>	log <i>K</i>	equilibrium quotient, <i>K'</i> , involving principal species	log <i>K'</i>
Bm	Cu	Py	H					
1	1	1	0	18.75(4)	[CuBmPy]/[CuBm][Py]	5.12	[CuBmPy]/[CuBm][Py]	5.12
1	1	1	1	27.99(3)	[CuBmHPy]/[CuBmH][Py]	6.07	[CuBmHPy]/[CuBm][HPy]	5.89
1	1	1	2	36.05(6)	[CuBmH <sub>2</sub> Py]/[CuBmH <sub>2</sub> ][Py]	6.87	[CuBmH <sub>2</sub> Py]/[CuBmH][HPy]	5.66
1	1	1	3	43.58(6)	[CuBmH <sub>3</sub> Py]/[CuBmH <sub>3</sub> ][Py]	10.68	[CuBmH <sub>3</sub> Py]/[CuBmH <sub>2</sub> ][HPy]	5.93
1	1	1	4	49.25(6)	[CuBmH <sub>4</sub> Py]/[CuBmH <sub>4</sub> ][HPy]	7.88	[CuBmH <sub>4</sub> Py]/[CuBmH <sub>2</sub> ][H <sub>2</sub> Py]	5.53
1	1	1	5	52.98(9)	[CuBmH <sub>5</sub> Py]/[CuBmH <sub>5</sub> ][H <sub>2</sub> Py]	5.54	[CuBmH <sub>5</sub> Py]/[CuBmH <sub>3</sub> ][H <sub>2</sub> Py]	5.54
1	2	1	-2	10.67(9)	[Cu <sub>2</sub> Bm(OH) <sub>2</sub> Py]/[Cu <sub>2</sub> Bm(OH) <sub>2</sub> ][Py]	2.75	[Cu <sub>2</sub> Bm(OH) <sub>2</sub> Py]/[Cu <sub>2</sub> Bm(OH) <sub>2</sub> ][Py]	2.75
1	2	1	-1	23.20(4)	[Cu <sub>2</sub> Bm(OH)Py]/[Cu <sub>2</sub> Bm(OH)][Py]	6.55	[Cu <sub>2</sub> Bm(OH)Py]/[Cu <sub>2</sub> Bm(OH)][Py]	6.55
1	2	1	0	32.26(2)	[Cu <sub>2</sub> BmPy]/[Cu <sub>2</sub> Bm][Py]	7.78	[Cu <sub>2</sub> BmPy]/[Cu <sub>2</sub> Bm(OH)][HPy]	7.14
1	2	1	1	39.38(4)	[Cu <sub>2</sub> BmHPy]/[Cu <sub>2</sub> Bm][HPy]	6.43	[Cu <sub>2</sub> BmHPy]/[Cu <sub>2</sub> Bm][HPy]	6.43
1	2	1	2	44.32(2)	[Cu <sub>2</sub> BmH <sub>2</sub> Py]/[Cu <sub>2</sub> Bm][H <sub>2</sub> Py]	5.30	[Cu <sub>2</sub> BmH <sub>2</sub> Py]/[Cu <sub>2</sub> Bm][H <sub>2</sub> Py]	5.30

<sup>a</sup> μ = 0.10 M (KCl); 25.0 °C (standard deviations in parentheses).

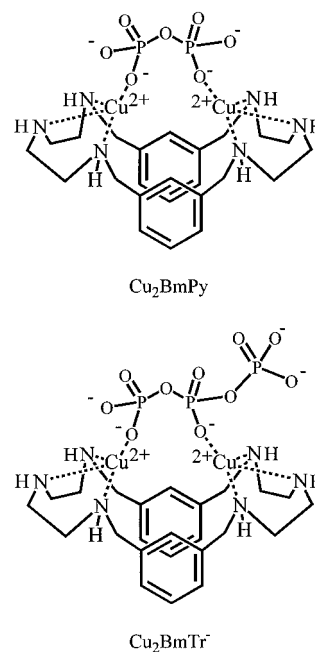
1. It is obvious that addition of a proton to Cu<sub>2</sub>BmHPh<sup>2+</sup> must necessarily decrease the strength of coordinate bonding and lead to a decrease in stability.

**Copper–BMXD–Pyrophosphate.** Table 5 gives the equilibrium constants for the interactions of 1 and 2 equiv of Cu<sup>2+</sup> with BMXD and pyrophosphate anion.

With 1 equiv of Cu<sup>2+</sup> the formation constants of the ternary species increase with increasing protonation of the mononuclear complex down the series from CuBmPy<sup>2-</sup> to CuBmH<sub>3</sub>Py<sup>+</sup>. This is due to the increase in electrostatic attraction between the mononuclear macrocyclic complex and the pyrophosphate anion and also because of the increasing hydrogen-bonding opportunities available. Beyond the species CuBmH<sub>3</sub>Py<sup>+</sup> the formation constants decrease because further protonation, now of the pyrophosphate anion, compromises the already optimum number of hydrogen-bonding interactions and also weakens the coordinate bond that the anion forms with the metal ion.

The stabilities of the dinuclear ternary species also initially increase with increasing protonation. The least stable species is Cu<sub>2</sub>Bm(OH)<sub>2</sub>Py<sup>2-</sup>, which is easily understood when one considers the strong affinity Cu<sub>2</sub>Bm<sup>4+</sup> has for hydroxide ions. As the p[H] is lowered the electrostatic attraction between the negatively charged pyrophosphate anion and the macrocyclic complex increases due to the increasing positive charge of the macrocyclic complex, giving rise to the larger formation constants of the species Cu<sub>2</sub>Bm(OH)Py<sup>-</sup> over that of Cu<sub>2</sub>Bm(OH)<sub>2</sub>Py<sup>2-</sup> and of Cu<sub>2</sub>BmPy over that of Cu<sub>2</sub>Bm(OH)Py<sup>-</sup>. A possible coordination mode for Cu<sub>2</sub>BmPy is depicted in Chart 2. Further increase of the degree of protonation results in protonation of the pyrophosphate anion in the complex. This decreases its basicity and the Coulombic attraction between itself and the dinuclear copper complex, resulting in the decreasing log formation constants that are seen for Cu<sub>2</sub>BmHPy<sup>+</sup> and Cu<sub>2</sub>BmH<sub>2</sub>Py<sup>2+</sup>.

Figure 2 shows the distribution of species as a function of p[H] for a solution containing BMXD, Cu<sup>2+</sup>, PO<sub>4</sub><sup>3-</sup>, and P<sub>2</sub>O<sub>7</sub><sup>4-</sup>

**Chart 2**

in a 1:2:1:1 ratio. The diagram demonstrates the competition between the ortho- and pyrophosphate anions for the dinuclear copper complex. Clearly the macrocyclic complex shows a much higher affinity for the pyrophosphate anion between p[H] 3 and 9 with orthophosphate ternary species accounting for less than 10% of the total ternary species present. Not until a p[H] of above 11 does the dinuclear copper(II) complex bind orthophosphate ion, in the form of Cu<sub>2</sub>Bm(OH)Ph, to a greater extent than pyrophosphate ion. At this p[H] however the total amount of ternary species decreases rapidly with p[H], giving way to the bis- and tris(hydroxo) binary species (not shown).

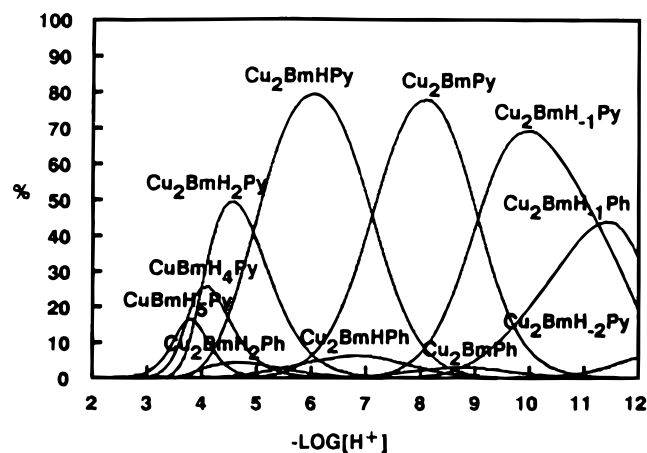


**Figure 2.** Distribution diagram showing the species formed as a function of  $p[H]$  when  $1.0 \times 10^{-3}$  M BMXD·6HBr,  $2.0 \times 10^{-3}$  M  $\text{CuCl}_2$ ,  $1.0 \times 10^{-3}$  M  $\text{PO}_4^{3-}$ , and  $1.0 \times 10^{-3}$  M  $\text{P}_2\text{O}_7^{4-}$  are equilibrated at 25.0 °C and  $\mu = 0.10$  M (KCl). Only the ternary complex species are shown. (Bm = BMXD; Ph =  $\text{PO}_4^{3-}$ ; Py =  $\text{P}_2\text{O}_7^{4-}$ ).

The results demonstrate that between certain  $p[H]$  regions the dinuclear copper(II) complex is able to selectively bind pyrophosphate ions in the presence of orthophosphate ions. This phenomenon is probably due to the ability of the pyrophosphate ion to offer a mode of coordinate bonding to the dicopper center which involves less steric strain through the macrocyclic backbone than does orthophosphate ion (see Chart 2).

**Copper–BMXD–Tripolyphosphate.** As in the absence of metal ions,<sup>13</sup> the tripolyphosphate anion shows the strongest interaction with the mononuclear and dinuclear copper(II) complexes of BMXD of all the phosphate type anions studied. Table 6 gives the results for overall and stepwise formation constants obtained from titrations of 1 and 2 equiv of  $\text{Cu}^{2+}$  with 1 equiv of BMXD and sodium tripolyphosphate.

The rearrangement of overall stability constants into the equilibrium quotient  $K$  demonstrates the increase in stability that is achieved as the degree of protonation of the mononuclear macrocyclic complex occurs. The increase in  $\log K$  reaches a maximum for the species  $\text{CuBmH}_3\text{Tr}$  which, as for the previous substrates, represents the optimum of hydrogen-bonding interactions and Coulombic attraction. The decrease in formation constants for the next two mononuclear species involving further protonation follow the trends seen in the case of both ortho- and pyrophosphate except that the magnitude of the decrease is much smaller. This indicates that further protonation of the tripolyphosphate ion has a much lesser effect upon the stability of the resulting ternary complex than it does for the other two substrates. This would seem to indicate that, unlike the case with ortho- or pyrophosphate ions, the addition of further protons to the tripolyphosphate anion does not disrupt any existing hydrogen bonding interactions or weaken the coordinate bond to the metal but instead protonation of an oxygen atom on the “free” end of the anion is occurring. In the absence of an X-ray crystal structure the mode of binding of the tripolyphosphate anion to the mononuclear copper(II) complex can only be speculated, but it would seem plausible that the oxygen atoms involved in binding to the mononuclear complex are those of one terminus and the central phosphate oxygen atom.

The complexes formed between the tripolyphosphate ion and the dinuclear copper(II) complex increase in stability as the degree of protonation of the copper(II) complex increases, reaching a maximum with the interaction of  $\text{Cu}_2\text{Bm}^{4+}$  and  $\text{Tr}^{5-}$ . A possible binding mode of the tripolyphosphate anion in the species  $\text{Cu}_2\text{BmTr}^-$  is shown in Chart 2. The formation constants for the species  $\text{Cu}_2\text{BmHTr}$  and  $\text{Cu}_2\text{BmH}_2\text{Tr}^+$  decrease

since the reacting species are now the protonated tripolyphosphate ions which have a lesser negative charge, but this decrease is not as marked as that with ortho- or pyrophosphate ion. If the coordination of the tripolyphosphate ion to the dinuclear metal center involves the central phosphate residue and one terminus, it can be postulated that the protonation is occurring on the free terminus of the tripolyphosphate anion as this would have a lesser effect on the coordinate bonding of the anion to the copper centers than it would if the oxygen atoms adjacent to those involved in coordination were being protonated.

The species distribution diagram showing the binding selectivity of the dinuclear copper(II) complex for either pyro- or tripolyphosphate ion as a function of  $p[H]$  is given in Figure 3. It is immediately apparent that the selectivity demonstrated for these two substrates is not as one-sided as that of pyrophosphate over orthophosphate (Figure 2). Between  $p[H]$  4 and 9.3 the dinuclear copper complex prefers to bind the tripolyphosphate ion, possibly because of its higher negative charge, but the discrimination is not complete as large amounts of pyrophosphate ternary species are also present. Above  $p[H]$  9.3 the pyrophosphate containing ternary species predominate over the tripolyphosphate species. As the  $p[H]$  is increased further all ternary species diminish in favor of hydroxo binary species. The ternary species present above  $p[H]$  9.3 also contain an hydroxide ion, probably bridging the metal centers, so there would be less electrostatic repulsion between this bridged hydroxide complex and the pyrophosphate ion than the tripolyphosphate ion. By adjusting the  $p[H]$  of such a mixture of components, one can control the relative proportions of pyrophosphate-bound complexes to tripolyphosphate-bound complexes and hence the selectivity of the system.

#### Equilibrium Constants Based on Main Species In Solution.

The above discussion of the association (recognition) constants are based on the affinities of the mononuclear and dinuclear copper(II) macrocyclic complexes for the most basic (most fully deprotonated) forms of the anions. When the copper(II) macrocyclic complex is fully protonated, the proton being added must necessarily be carried by the anion. Thus for the mononuclear complexes Tables 4–6 show the stepwise association constants of the copper(II) macrocyclic complexes with the most basic forms of the anions as the degree of protonation increases, and the trends are rationalized on the basis of hydrogen bonding and Coulombic effects. This procedure is analogous to the use of stability constants whereby the affinity of the ligand in its most basic form is employed although that form frequently does not occur, except at very high pH.

It is also possible to express the equilibrium constants in terms of the most important form of the anion that exists under conditions where the tertiary complex species is formed. These equilibrium constants are given in the last two columns of Tables 4–6 and may be calculated from the other constants listed by use of the protonation constants of the anion. The trends in the stepwise constants listed in Tables 4–6 based on the principal species in solution are generally the same as those of the stepwise constants based on the most basic form of the anion when the principal species of the anion remains the same. The constants in Table 4 for the binding of  $\text{HPO}_4^{2-}$  increase as the number of protons bound increases. When the latter is changed, as in the binding of  $\text{H}_2\text{PO}_4^-$  in place of  $\text{HPO}_4^{2-}$ , there is a discontinuity in the stepwise constants. Thus the two correlations of the stepwise constants in Tables 4–6 are the same, if the degree of protonation of the anionic species is taken into account.

**Table 6.** Overall Stability Constants and Stepwise Formation Constants for the Cu(II)–BMXD–Tripolyphosphate System (Bm = BMXD; Tr =  $P_3O_{10}^{5-}$ ; Charges Have Been Omitted for Clarity)

stoichiometry				$\log \beta^a$	equilibrium quotient, $K$	$\log K$	equilibrium quotient, $K'$ , involving principal species	$\log K'$
Bm	Cu	Tr	H					
1	1	1	0	18.50(3)	[CuBmTr]/[CuBm][Tr]	4.87	[CuBmTr]/[CuBm][Tr]	4.87
1	1	1	1	27.81(1)	[CuBmHTr]/[CuBmH][Tr]	5.89	[CuBmHTr]/[CuBm][HTr]	6.11
1	1	1	2	36.46(3)	[CuBmH <sub>2</sub> Tr]/[CuBmH <sub>2</sub> ][Tr]	7.28	[CuBmH <sub>2</sub> Tr]/[CuBmH][HTr]	6.47
1	1	1	3	44.18(2)	[CuBmH <sub>3</sub> Tr]/[CuBmH <sub>3</sub> ][Tr]	11.28	[CuBmH <sub>3</sub> Tr]/[CuBmH <sub>2</sub> ][HTr]	6.93
1	1	1	4	50.18(1)	[CuBmH <sub>4</sub> Tr]/[CuBmH <sub>4</sub> ][Tr]	9.21	[CuBmH <sub>4</sub> Tr]/[CuBmH <sub>2</sub> ][H <sub>2</sub> Tr]	7.40
1	1	1	5	54.35(1)	[CuBmH <sub>5</sub> Tr]/[CuBmH <sub>5</sub> ][H <sub>2</sub> Tr]	7.85	[CuBmH <sub>5</sub> Tr]/[CuBmH <sub>3</sub> ][H <sub>2</sub> Tr]	7.85
1	2	1	-2	11.51(4)	[Cu <sub>2</sub> Bm(OH) <sub>2</sub> Tr]/[Cu <sub>2</sub> Bm(OH) <sub>2</sub> ][Tr]	3.59	[Cu <sub>2</sub> Bm(OH) <sub>2</sub> Tr]/[Cu <sub>2</sub> Bm(OH) <sub>2</sub> ][Tr]	3.59
1	2	1	-1	22.73(1)	[Cu <sub>2</sub> Bm(OH)Tr]/[Cu <sub>2</sub> Bm(OH)][Tr]	6.08	[Cu <sub>2</sub> Bm(OH)Tr]/[Cu <sub>2</sub> Bm(OH)][Tr]	6.08
1	2	1	0	32.53(4)	[Cu <sub>2</sub> BmTr]/[Cu <sub>2</sub> Bm][Tr]	8.05	[Cu <sub>2</sub> BmTr]/[Cu <sub>2</sub> Bm][HTr]	7.81
1	2	1	1	39.75(1)	[Cu <sub>2</sub> BmHTr]/[Cu <sub>2</sub> BmH][Tr]	7.20	[Cu <sub>2</sub> BmHTr]/[Cu <sub>2</sub> Bm][HTr]	7.20
1	2	1	2	44.96(3)	[Cu <sub>2</sub> BmH <sub>2</sub> Tr]/[Cu <sub>2</sub> BmH <sub>2</sub> ][Tr]	6.88	[Cu <sub>2</sub> BmH <sub>2</sub> Tr]/[Cu <sub>2</sub> Bm][H <sub>2</sub> Tr]	6.88

<sup>a</sup>  $\mu = 0.10$  M (KCl); 25.0 °C (standard deviations in parentheses).

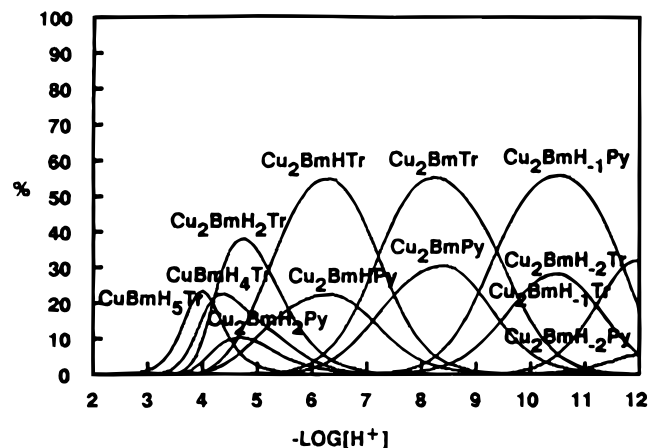


**Figure 3.** Distribution diagram showing the species formed as a function of  $p[H]$  when  $1.0 \times 10^{-3}$  M BMXD·6HBr,  $2.0 \times 10^{-3}$  M CuCl<sub>2</sub>,  $1.0 \times 10^{-3}$  M  $P_2O_7^{4-}$ ,  $1.0 \times 10^{-3}$  M  $P_3O_{10}^{5-}$  are equilibrated at 25.0 °C and  $\mu = 0.10$  M (KCl). Only the ternary complex species are shown. (Bm = BMXD; Py =  $P_2O_7^{4-}$ ; Tr =  $P_3O_{10}^{5-}$ ).

## Conclusion

These results show that both the mono- and dinuclear copper(II) complexes of BMXD are able to act as hosts for the series of phosphate anions. For all the anions studied it was found that the dinuclear copper(II) complex of BMXD,  $Cu_2Bm^{4+}$ , is able to bind each of the anions with a greater stability constant than the hydroxo-bridged dinuclear copper(II) complexes; however, the mononuclear copper(II) complexes of BMXD are able to form a greater number of ternary species of fairly uniform (and high) stability. This is not surprising since the interactions between the anions and the dinuclear copper(II) complexes are aided by electrostatic forces which are naturally dependent on the charges of each individual reacting species, whereas the interactions between the anions and the mononuclear copper(II) complexes are amplified by the electrostatic attractive forces as well as the formation of hydrogen bonds between the oxygen atoms of the phosphate residues and the protonated amino nitrogen atoms of the macrocycle.

In the absence of metal ions, the triphosphate anion forms binary complexes with BMXD of much greater stability than those formed between pyrophosphate and BMXD.<sup>13</sup> In the presence of  $Cu^{2+}$  the stability of triphosphate ternary complexes are the same or slightly greater than those of pyrophosphate. Because the coordination of a copper(II) ion

to BMXD involves three amino nitrogen atoms, as shown by the X-ray structural results of  $(Cu_2-BMXD)(SO_4)_2$ , these nitrogen atoms therefore are not available for hydrogen bonding. This loss in H-bonding opportunities affects triphosphate more than pyrophosphate since it possesses the greater number of negative oxygen atoms.

The spatial disposition of the copper(II) center and the remaining amino nitrogen atoms in the mononuclear complex, and also the two copper(II) centers in the dinuclear complex, may be such as to be well suited to the incorporation of anions of size equivalent to pyrophosphate. Anions of this size have already been demonstrated as forming strong interactions with metal complexes of similar macrocycles.<sup>4,9,32</sup> It may well be the case that triphosphate anion is forced to coordinate to the host complex in a manner similar to pyrophosphate, as suggested in Chart 2. This would therefore explain the similar stabilities found for the ternary complexes of both these anions.

The dinuclear copper(II) complexes of BMXD are able to selectively bind pyrophosphate ions in the presence of orthophosphate ions over the whole  $p[H]$  range in which these ternary interactions are important. However the selectivity shown for pyrophosphate ions in the presence of triphosphate ions is  $p[H]$  dependent. The binding of phosphate, pyrophosphate, and triphosphate anions to the copper(II) complexes of BMXD continues up to a much higher  $p[H]$  than is the case in the absence of metal ions.<sup>13</sup> This, and the fact that the structure of the ternary species may be of the form suggested for  $Cu_2BmTr^-$ , Chart 2, has important implications in the design of molecular catalysts for effecting reactions that involve nucleophilic attack by hydroxide ion. Already the macrocycles BMXD and OBISDIEN have been shown to catalyze the hydrolysis of ATP at low  $p[H]$  (<8), but the catalysis of such reactions has not been demonstrated at higher  $p[H]$ .<sup>7,33</sup> Metal complexes, such as those studied here, may prove to be suitable for substrate binding and catalysis over a wide  $p[H]$  range.

**Acknowledgment.** This work was supported by the Robert A. Welch Foundation under Grant No. A-259.

**Supporting Information Available:** Supporting information comprising atomic coordinates and equivalent isotropic displacement parameters for  $(Cu_2-BMXD)(SO_4)_2$ , Table SI, anisotropic displacement parameters, Table SII, and hydrogen atom coordinates, Table SIII (3 pages). Ordering information is given on any current masthead page.

IC960661Q

(33) Nation, D. A.; Martell, A. E. Manuscript in preparation.